

Research Article

Open Access



# A hierarchical design for thermoelectric hybrid materials: Bi<sub>2</sub>Te<sub>3</sub> particles covered by partial Au skins enhance thermoelectric performance in sticky thermoelectric materials

Norifusa Satoh\*, Masaji Otsuka, Jin Kawakita, Takao Mori

National Institute for Materials Science, Tsukuba 305-0044, Japan.

\*Correspondence to: Dr. Norifusa Satoh, National Institute for Materials Science, Tsukuba 305-0044, Japan.  
E-mail: SATOH.Norifusa@nims.go.jp

**How to cite this article:** Satoh N, Otsuka M, Kawakita J, Mori T. A hierarchical design for thermoelectric hybrid materials: Bi<sub>2</sub>Te<sub>3</sub> particles covered by partial Au skins enhance thermoelectric performance in sticky thermoelectric materials. *Soft Sci* 2022;2:15. <https://dx.doi.org/10.20517/ss.2022.15>

**Received:** 14 Jul 2022 **First Decision:** 18 Jul 2022 **Revised:** 8 Aug 2022 **Accepted:** 12 Aug 2022 **Published:** 1 Sep 2022

**Academic Editor:** Zhifeng Ren **Copy Editor:** Fangling Lan **Production Editor:** Fangling Lan

## Abstract

Sticky thermoelectric (TE) materials have been inversely designed to enable the mass production of flexible TE sheets through lamination or roll-to-roll processes without using electrically conductive adhesives. They have also been demonstrated as inorganic/organic hybrid materials consisting of TE inorganic particles and low-volatilizable organic solvents to exhibit Seebeck coefficients based on the TE particles and low thermal conductivities based on the organic matrix. To achieve energy harvesting of 250  $\mu$ W for driving various electric devices using voltage boosters, herein, we employ p- and n-type Bi<sub>2</sub>Te<sub>3</sub> particles due to their high Seebeck coefficients, and cover the Bi<sub>2</sub>Te<sub>3</sub> bodies with Au skins because the interfacial electrical resistance depends on the electrical resistance of opposing substances at the interface. After controlling the plating amount to cover the Bi<sub>2</sub>Te<sub>3</sub> particles with Au skins, we achieve a TE power generation two orders of magnitude greater than the previous study, i.e., 255  $\mu$ W on a hot plate of 110 °C with a 6 × 6 module. Overall, with input from other organic devices, like organic light-emitting diodes and dye-sensitized solar cells, this study presents a hierarchical design for TE hybrid materials that suppresses the thermal conduction by hybridizing TE particles with the organic matrix at the microscale. This reduces the electrical resistance by modifying the interfaces of the TE particles at the nanoscale and optimizes the Seebeck coefficient of TE particles at the atomic scale. To compete with solid-state TE modules with regards to power generation capacity, the hierarchical design towards a possible further two orders of magnitude improvement is also discussed.



© The Author(s) 2022. **Open Access** This article is licensed under a Creative Commons Attribution 4.0 International License (<https://creativecommons.org/licenses/by/4.0/>), which permits unrestricted use, sharing, adaptation, distribution and reproduction in any medium or format, for any purpose, even commercially, as long as you give appropriate credit to the original author(s) and the source, provide a link to the Creative Commons license, and indicate if changes were made.



**Keywords:** Hybrid materials,  $\text{Bi}_2\text{Te}_3$  particles, particle plating, hierarchical design, organic light-emitting diodes, dye-sensitized solar cells

## INTRODUCTION

Compared with solid-state thermoelectrics (TEs), soft TEs have decisive advantages in that they can fit the various shapes of heat sources and absorb thermal energy efficiently. Due to the strong demands for energy harvesting, organics and inorganic/organic hybrids have been widely investigated as soft TE materials<sup>[1-3]</sup>. One target value for energy harvesting is 250  $\mu\text{W}$ , which can be used to drive various electric devices using commercially available voltage boosters. However, when progressing to applications, there is a general difficulty in making electrical contacts between the soft TE materials and electrodes because we cannot simply apply the traditional method for solid-state TEs, i.e., soldering, to soft TEs due to the low thermostability of organics<sup>[4]</sup>.

As a possible solution to making electrical contacts based on materials design, we presented a working hypothesis of sticky TE materials to contact with the electrodes by themselves and enable the mass production of flexible TE sheets through lamination or roll-to-roll processes without using electrically conductive adhesives [Figure 1]<sup>[4]</sup>. The concept of sticky TE materials has been demonstrated using inorganic/organic hybrid materials of TE particles with low-volatilizable organic solvents, which exhibit Seebeck coefficients based on the TE particles and low thermal conductivities based on the organic matrix<sup>[5]</sup>. The previous result suggests that the structural parameters in the TE modules may be able to compensate for the physical property limitations in TE materials, i.e., the thermal-insulating surroundings can modulate the thermal conductivity of TE materials extrinsically. However, the first sticky TE materials only generated 2.1  $\mu\text{W}$  on a hot plate of 120 °C with a 6 × 6 module because of the high interfacial electrical resistance between the TE particles, even though they are metallic like Sb (0.4  $\mu\Omega\text{m}$ ) for the p-type material and Bi (1.3  $\mu\Omega\text{m}$ ) for the n-type material. The Seebeck coefficients of these materials are also relatively small, i.e., 35  $\mu\text{V/K}$  for Sb and -70  $\mu\text{V/K}$  for Bi.

To enhance the TE power generation, herein, we employ p- and n-type  $\text{Bi}_2\text{Te}_3$  particles due to their high Seebeck coefficients ( $\sim\pm 150 \mu\text{V/K}$ ) and cover the  $\text{Bi}_2\text{Te}_3$  bodies with Au skins (22  $\text{n}\Omega\text{m}$ ) because the interfacial electrical resistance depends on the electrical resistances of the opposing substances opposing at the interface. As a result, we divide the two requirements for the TE particles, namely, a high Seebeck coefficient and low interfacial resistance, into the two material components of the  $\text{Bi}_2\text{Te}_3$  bodies and the Au skins, respectively. Furthermore, typically, in bulk TE materials, all-scale hierarchical architectures scatter multiscale wavelength phonons to reduce the thermal conductivity<sup>[6,7]</sup>. In contrast, for sticky TE materials, the low-volatilizable organic solvent matrix provides low thermal conductivity.

Our materials design is inspired by other organic devices, such as organic light-emitting diodes (OLEDs)<sup>[8]</sup> and dye-sensitized solar cells (DSCs)<sup>[9,10]</sup> [Figure 2]. OLEDs accept organic multiple layer structures consisting of electron-injection, hole-injection and light-emitting layers because single organic layers by themselves cannot easily meet all of the functional requirements, including hole and electron injection and hole-electron recombination to emit light [Figure 2A]. In DSCs, the multiple components are able to exhibit superior photovoltaic characteristics, where a dye molecule absorbs light to generate a hole-electron pair and then the  $\text{I}^-/\text{I}_3^-$  electrolyte solution and  $\text{TiO}_2$  separately transfer the hole and electron to the external circuit [Figure 2B]. Similar to OLEDs and DSCs, sticky TE materials consist of individually-acting components, such as low-volatilizable organic solvents and sealants to suppress the thermal conduction, Au skins to reduce the electrical resistance and  $\text{Bi}_2\text{Te}_3$  bodies to generate the thermopower, controlled

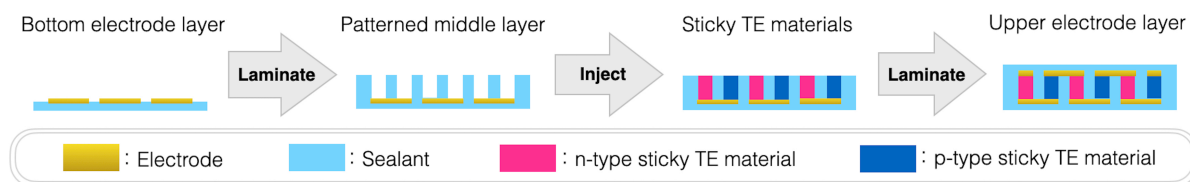


**Figure 1.** Schematic of the three-step fabrication process of sticky TE modules. TE: Thermoelectric.

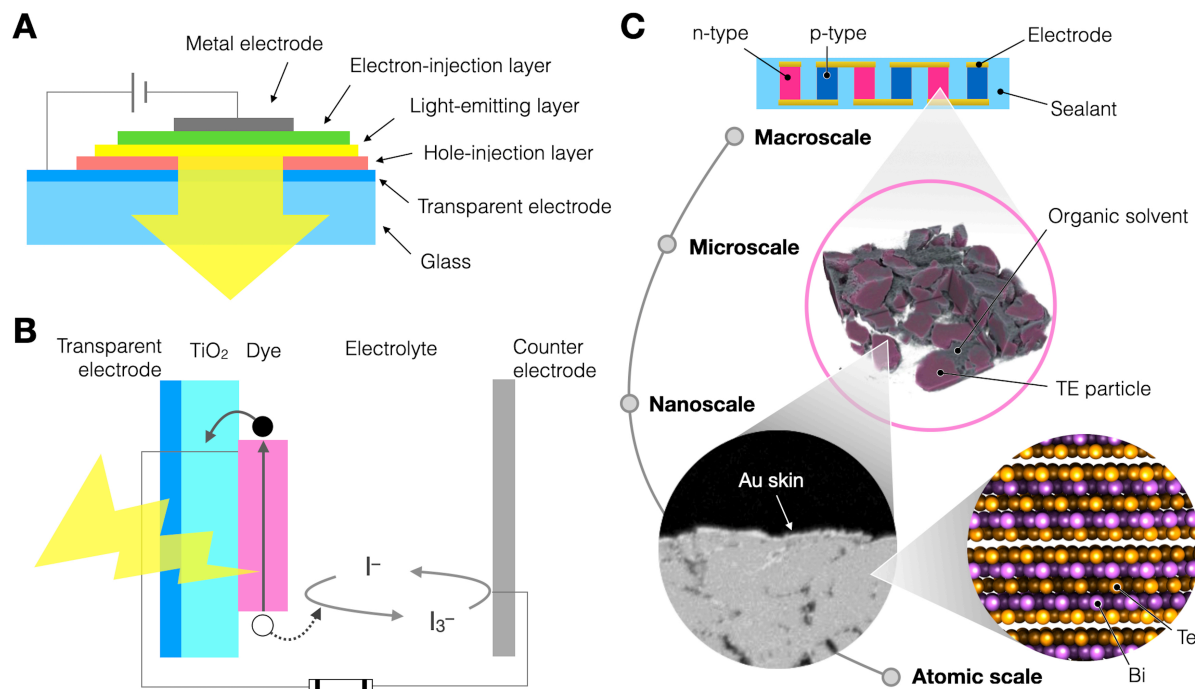


**Figure 2.** (A) Schematic device structure of OLEDs; (B) schematic energy diagram of DSCs; (C) schematic of hierarchical design for sticky TE materials. OLEDs: Organic light-emitting diodes; DSCs: dye-sensitized solar cells.

hierarchically at the microscale, nanoscale and atomic scale, respectively [Figure 2C].

When characterizing the as-fabricated sticky TE materials, we enclose the sticky TE materials within a single cell (diameter of 3 mm and height of 3 mm) as part of the module structure contacted with the top and bottom electrodes and surrounded with a sealant material. This is because commercial measurement systems have been designed for solid-state TE materials and not for deformable materials like sticky TE materials. Although we separately prepared an original measurement capsule to set inside the commercial measurement system, a ZEM-3 (ADVANCE RIKO, Inc.), and tried to characterize the individual thermoelectric properties, we could not perform favorable electrical analyses because the performance depends on the pressure applied on the samples. The pressure affects the contact area between the TE particles, thereby defining the interfacial electrical resistance. In contrast, in the single cell, the pressure is controlled by the volume ratio of the sticky TE materials to the cell, which is nearly one in this case. Consequently, the single-cell measurement method is of particular value for the practical design of module structures because the obtained data using the single-cell structures include the features of the contact resistance between the sticky TE materials and electrodes and the thermal insulation effects from the organic matrix.

In this study, we investigate the necessary plating amount to cover the  $\text{Bi}_2\text{Te}_3$  particles with Au skins using a single cell and then demonstrate the efficiency of this strategy by achieving a TE power generation two orders of magnitude greater than the previous study of  $255 \mu\text{W}$  on a hot plate of  $110 \text{ }^\circ\text{C}$  with the  $6 \times 6$  module. The module size and thickness are designed to compare the performance with commercially available solid-state TE modules of the same dimensions. Although the obtained energy harvesting of  $250 \mu\text{W}$  drives various electric devices using voltage boosters, the power generation capacity is still lower than that of commercially available solid-state TE modules<sup>[11-13]</sup>. With the aim of achieving a further two orders of magnitude improvement, we also discuss the further possibilities of sticky TE materials to enhance the TE performance.

## EXPERIMENTAL

The p- and n-type  $\text{Bi}_2\text{Te}_3$  particles meshed for 75-150 and 150-300  $\mu\text{m}$  were purchased from Toshima Manufacturing Co., Ltd., Japan. The original Seebeck coefficients and electrical conductivities were confirmed before usage to be in the range of 133-155  $\mu\text{V/K}$  and 7.86-9.05  $\mu\Omega\text{m}$  for p-type  $\text{Bi}_2\text{Te}_3$  and -138-143  $\mu\text{V/K}$  and 9.95-11.9  $\mu\Omega\text{m}$  for n-type  $\text{Bi}_2\text{Te}_3$ , respectively. The corresponding power factors were 2.16-2.81  $\text{mW/mK}^2$  for p-type  $\text{Bi}_2\text{Te}_3$  and 1.67-1.94  $\text{mW/mK}^2$  for n-type  $\text{Bi}_2\text{Te}_3$ . The displacement Au plating of these TE particles was performed and characterized by Kiyokawa Plating Industry Co., Ltd., Japan. Before mixing with the Au skin-covered  $\text{Bi}_2\text{Te}_3$  powders, palm shortening (trans-fat free, Daabon, Colombia) was heated under a vacuum at  $60 \text{ }^\circ\text{C}$  for 30 min. The vacuum-dried shortening was added to the Au skin-covered  $\text{Bi}_2\text{Te}_3$  powders at a volume ratio of 50% to prepare the sticky TE materials. The copper-clad flexible films (F-30VC1, Nikkan Industries Co., Ltd., Japan) were pattern etched and plated to prepare the upper and bottom electrodes. As the middle layer, both sides of the 3-mm-thick polyurethanes (Kyushu Packing Co., Ltd., Japan) were laminated with double-coated adhesive tapes (HJ-9150W, Nitto Denko, Japan), patterned with a laser-cutting machine (VLS2.30DT, Universal Laser Systems, USA), cleaned with acetone and dried under a vacuum. After the underside of the middle layers was sealed with the bottom electrode films, the sticky TE materials were injected into the patterned holes. The top surfaces of the middle layers were sealed with the upper electrode films.

The thermopower ( $V$ ) and temperature difference ( $\Delta T$ ) were monitored to read the stabilized value with a data logger (LR8432, Hioki E.E. Corporation, Japan), where the bottom sides were heated with an air-cooling Peltier plate (CHP-77HI, Sensor Controls Co., Ltd., Japan) and the upper side was naturally cooled by air with a fin (height of 1 cm). The resistance ( $R$ ) was measured at room temperature with a digital multimeter (CDM-2000D, CUSTOM, Japan). The current-voltage ( $I$ - $V$ ) curves were obtained by plotting the  $V$  measured with the data logger after being stabilized during the input of several different  $I$  into the sticky TE modules with the current source (GS200, Yokogawa Electric Corporation, Japan) placed on the air-cooling Peltier plate set at 60 and  $110 \text{ }^\circ\text{C}$  and cooled naturally by air with a fin (height of 2 cm). To compare the performance, a solid-state TE module of the same size (TEC1-12706, 4 cm  $\times$  4 cm) was purchased.

## RESULTS AND DISCUSSION

The characteristics of the Au skin-covered  $\text{Bi}_2\text{Te}_3$  particles and the sticky TE performance on the single cell are summarized in Table 1. The Au skins on both the p- and n-type  $\text{Bi}_2\text{Te}_3$  particles reduce the  $R$  but also decrease the  $\Delta T$  because of the heat conduction. Thus, Au skins with a thickness of  $< 100 \text{ nm}$  enhance the power generation ( $V^2/4R$ ), whereas thicknesses of  $> 100 \text{ nm}$  decrease the performance. From the large drop in voltage for the large Au skin plating weight, i.e., thickness, it can be surmised that the Au skins become more thermally percolating, thereby degrading the Seebeck voltage.

**Table 1. Characteristics of Au skin-covered Bi<sub>2</sub>Te<sub>3</sub> particles and sticky TE performance in a single cell measured on a hotplate of 60 °C with a fin**

Type	Size (μm)	Plating weight (wt.%)	Cross-sectional thickness (nm)*	R (Ω)	V (mV)	V <sup>2</sup> /4R (μW)	ΔT (°C)
p	150-75	0	-	2.4	1.02	0.11	18
		1.00	-	0.8	1.12	0.39	17
		6.51	47	0.4	0.91	0.52	15
	300-150	0	-	3.5	1.25	0.11	18
		2.76	66	0.7	1.62	0.94	17
		4.91	109	0.3	0.51	0.22	13
n	150-75	0	-	2.3	-0.87	0.08	18
		0.28	-	1.4	-1.15	0.24	16
		7.23	25	0.6	-1.09	0.49	14
	300-150	0	-	0.5	-1.12	0.13	18
		2.23	50	0.5	-1.29	0.84	17
		3.86	119	0.4	-0.59	0.22	12

\*Representative value. The actual value depends on the measuring points, especially for the partial Au skins.

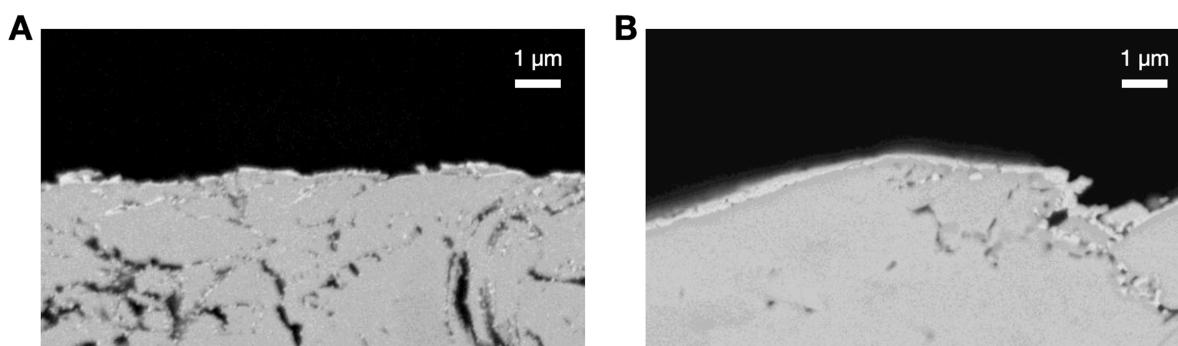


**Figure 3.** Cross-sectional SEM images comparing the partial and full Au skins. (A) Partial Au skin: 300 μm p-type Bi<sub>2</sub>Te<sub>3</sub> particles with 2.76 wt.% Au skin; (B) full Au skin: 300 μm p-type Bi<sub>2</sub>Te<sub>3</sub> particles with 3.86 wt.% Au skin. SEM: Scanning electron microscopy.

The behavior of the temperature dependence, namely, the heat conduction, can be explained from cross-sectional scanning electron microscopy (SEM) images [Figure 3]. Geometrically assuming the full 50 nm Au skins on spherical dense p- and n-type Bi<sub>2</sub>Te<sub>3</sub> particles of 150 and 300 μm in diameter, we expected a plating weight of less than 1 wt.% for all of them. Experimentally, however, the partial 50 nm Au skins required plating weights of 6.51 and 7.23 wt.% for the 150 μm p- and n-type Bi<sub>2</sub>Te<sub>3</sub> particles and 2.76 and 2.23 wt.% for the 300 μm p- and n-type Bi<sub>2</sub>Te<sub>3</sub> particles, respectively, because of the excess amount of Au deposited inside the voids of the actual Bi<sub>2</sub>Te<sub>3</sub> particles. In the comparison between the partial 50 nm Au skin samples, the 300 μm p- and n-type Bi<sub>2</sub>Te<sub>3</sub> particles with 2.76 and 2.23 wt.% Au skin show higher ΔT than the 150 μm p- and n-type Bi<sub>2</sub>Te<sub>3</sub> particles with 6.51 and 7.23 wt.% Au skin, respectively, due to the lower Au composition [Table 1].

In contrast to the partial Au skins of 2.76 and 2.23 wt.% on the 300 μm p- and n-type Bi<sub>2</sub>Te<sub>3</sub> particles [Figure 3A], the 4.91 and 3.86 wt.% Au skins on the 300 μm p- and n-type Bi<sub>2</sub>Te<sub>3</sub> particles, respectively, fully cover the surface with over 100 nm in thickness [Figure 3B], showing the smallest ΔT even without the highest Au plating weight [Table 1]. This means that the full Au skins serve as heat conduction paths to reduce the ΔT. Note that V has no linear relation with ΔT mainly because of the varying Seebeck coefficients of the composites mentioned above and also because ΔT includes the temperature losses on the

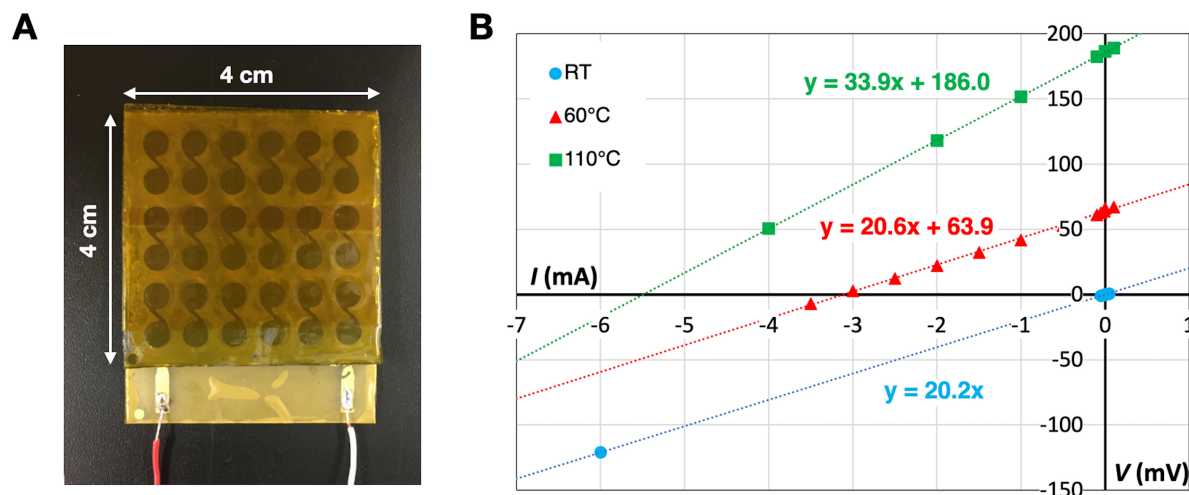


**Figure 4.** (A) External dimensions of a  $6 \times 6$  module. (B)  $I$ - $V$  characteristics of a  $6 \times 6$  module at RT,  $60^\circ\text{C}$  and  $110^\circ\text{C}$  under natural air cooling conditions with a fin.

top and bottom electrodes. In short, we observed the best TE performance with the partial Au skins on the  $300\ \mu\text{m}$  p- and n-type  $\text{Bi}_2\text{Te}_3$  particles [Table 1].

Based on the single-cell characteristics, herein, we can estimate the Seebeck coefficients and electrical resistivities for the sticky TE materials in this study. Using  $\Delta T$  measured from the outsides of the single-cell structures, the Seebeck coefficients of the best p- and n-type sticky TE materials are calculated to be  $95.3$  and  $-75.9\ \mu\text{V}/\text{K}$ , respectively. These values are relatively comparable to the original values before usage, considering the fact that  $\Delta T$  is overestimated by the temperature losses on the upper and bottom electrode sheets. The trend was also observed in the previous study (sticky Sb and sticky Bi:  $12$  and  $-40\ \mu\text{V}/\text{K}$  measured under the same conditions, against the literature values of Sb and Bi:  $35$  and  $-70\ \mu\text{V}/\text{K}$ )<sup>[5]</sup>. In contrast, the electrical resistivities increase by approximately two orders of magnitude. Using the measured diameters and heights of the single cells for estimating the volume of sticky TE materials that has been injected, we can simply calculate the electrical resistivities for the best p- and n-type sticky TE materials to be  $1.7$  and  $1.2\ \text{m}\Omega\text{m}$ , respectively. Note that these values include the interfacial electrical resistances with the upper and bottom electrodes because the single-cell analysis is a type of two-point probe method. Even so, this estimation suggests that there is still significant potential for improvement regarding electrical resistivity in future studies.

To demonstrate the progress of the materials design in this study, we fabricated a  $6 \times 6$  module structure using the sticky TE materials of partial Au skin-covered p- and n-type  $\text{Bi}_2\text{Te}_3$  particles of  $300\ \mu\text{m}$  [Figure 4A] and measured the  $I$ - $V$  characteristics at RT,  $60^\circ\text{C}$  and  $110^\circ\text{C}$  under natural air cooling conditions with a fin [Figure 4B]. The fabricated  $6 \times 6$  module showed  $R = 20.2\ \Omega$ , which is calculable from the  $R$  of the single cells and the numbers of cells in the module. The resistance is an order of magnitude lower than that of the previous module, showing the efficacy of the Au skin strategy<sup>[5]</sup>. We also confirmed  $R$  from the slope of the  $I$ - $V$  characteristics at RT. The  $I$ - $V$  curve for  $60^\circ\text{C}$  exhibited  $V^2/4R = 49.7\ \mu\text{W}$  based on  $R = 20.6\ \Omega$  as the slope and  $V = 63.9\ \text{mV}$  as the intercept with  $\Delta T = 20.4^\circ\text{C}$ , which represent values expected from the single-cell characteristics. More specifically, Seebeck coefficients can be calculated as an average of the absolute values for the p- and n-type sticky TE materials to be  $87.0$  and  $109.0\ \mu\text{V}/\text{K}$  from the  $I$ - $V$  curves at  $60$  and  $110^\circ\text{C}$ , respectively. The calculated values become closer to the original values as the  $\Delta T$  increases because the temperature actually applied on the sticky TE materials increases closer to  $\Delta T$  as the

temperature lost on the upper and bottom electrode sheets becomes more negligible. When increasing the temperature of the hot plate, we observed  $V^2/4R = 255 \mu\text{W}$  at  $110 \text{ }^\circ\text{C}$  with  $\Delta T = 47.4 \text{ }^\circ\text{C}$ . This performance is over two orders of magnitude higher than that of the previous sticky TE material module<sup>[5]</sup>.

To compare the current achievements with other organic and inorganic/organic hybrid TE modules, which have been reported in a range of  $5 \mu\text{W}/\text{cm}^2$  with  $\Delta T = 70 \text{ }^\circ\text{C}$  to  $4.1 \text{ mW}/\text{cm}^2$  with  $\Delta T = 60 \text{ }^\circ\text{C}$ ,<sup>[3]</sup> the observed power is converted to a power density, i.e.,  $16 \mu\text{W}/\text{cm}^2$  with  $\Delta T = 47.4 \text{ }^\circ\text{C}$ . Although some reports have achieved over two orders of magnitude higher power densities, their strategy involves the printing and postannealing at  $\sim 500 \text{ }^\circ\text{C}$  of  $\text{Bi}_2\text{Te}_3$  inks to grow the grains to approach bulk  $\text{Bi}_2\text{Te}_3$ .<sup>[14]</sup> In short, this comparison also suggests that sticky TE materials require further improvement regarding the interfacial electrical connection between the TE particles in order to achieve the performance of bulk  $\text{Bi}_2\text{Te}_3$ . In comparison with other works, the cycling bending on the current sticky TE modules breaks the upper electrode sheet before testing on the sticky TE materials. This is because the module is designed to be comparable with commercially available solid-state TE modules with the same dimensions, and in this case, the module thickness creates breaking tension on the electrode sheets.

To compete with other works and solid-state TE modules in terms of power generation capacity (the capacity of TEC1-12706 is  $R = 2.82 \Omega$ ,  $V = 158 \text{ mV}$  and  $V^2/4R = 2.21 \text{ mW}$  at  $60 \text{ }^\circ\text{C}$  and  $R = 3.33 \Omega$ ,  $V = 513 \text{ mV}$  and  $V^2/4R = 19.8 \text{ mW}$  at  $110 \text{ }^\circ\text{C}$ ), we can redesign the sticky TE materials at the macroscale, microscale, nanoscale and atomic scale from the bottom up. At the macroscale, we could increase the cell density per area to enhance the  $V^2/4R$ . Because both  $V$  and  $R$  increase with the cell number,  $V^2/4R$  also increases with the cell number. Under an assumption of constant single-cell resistance, regardless of the cell density and cell diameter, the high cell density tends to enhance the  $V^2/4R$  in general. Reducing the cell diameter from  $3.0$  to  $1.5 \text{ mm}$  and the cell pitch from  $6.0$  to  $2.5 \text{ mm}$ , we expect that the cell density could reach about five times higher, which is comparable with that of commercially available solid-state TE modules. Although the decrease in cell diameter may slightly increase the actual single-cell resistance, the cell number in the TE module, namely, the cell density, is one of the determining factors for the power generation capacity.

At the microscale, we can survey the combination between low-volatilizable organic solvents and sealants and improve these thermal stabilities to stabilize the TE performance in order to prevent the  $R$  increase with temperature, as observed here at  $110 \text{ }^\circ\text{C}$ . Simultaneously, we can replace the polyurethane sealants with thermal insulation foams because of the lower thermal conductivities, i.e.,  $0.21 \text{ W/mK}$  for polyurethane and  $0.023 \text{ W/mK}$  for thermal insulator foams. As an initial assessment, the thermal insulation foams generated twice as large  $\Delta T$  than polymer film sealants. One requirement for the foams is that the microscale pores must be a closed-cell type and smaller than the size of TE particles to serve as a sealant. Note that  $\Delta T$  depends on thermal conductivity and heat flux, but thermal insulator foams also reduce the heat flux. Thus,  $\Delta T$  does not seem to have a linear relation with thermal conductivity in this experimental setup. Nevertheless, the reduced heat flux contributes to improving the TE energy conversion efficiency from heat flux to electricity. The thermal insulation feature is further beneficial to make the flexible TE modules slimmer and lighter because the modules can more easily maintain  $\Delta T$  even for thin sheets. Moreover, the foam feature can buffer the mechanical stress to reduce the tension on the upper and bottom electrode sheets during cyclic bending.

At the nanoscale, we may be able to solder the TE particles with the Au skins by the method of electric resistance heating. The melting points of materials decrease with the reduction of size, especially at the nanoscale, because the ratio of bonding-free surface to solidified bodies increases<sup>[15]</sup>. Thus, the electric

resistance heating at the interfaces could melt the Au skins to solder TE particles with less typical damage to the organic matrix. Since the interfacial electrical resistance also depends on the contacting area at the interface, the one-time melted Au skins can fit with the shape of TE particles and reduce  $R$ . As a preliminary result, an order of magnitude reduction of  $R$  has been obtained with this method. From the perspective of material choice, Ag could be a better candidate for the conductive skins because of its lower electrical resistance (16 nΩm) and lower price (~1/100).

In addition to the expected two orders of magnitude improvement above, we can also optimize the particular property composition of the Bi<sub>2</sub>Te<sub>3</sub> particles at the atomic scale to better match the conditions for sticky TE materials. Solid-state TE materials typically need to optimize three correlating properties, i.e., the Seebeck coefficient, electrical resistivity and thermal conductivity, to maximize the TE performance. In contrast, the TE particles for the sticky TE materials mainly need to consider Seebeck coefficient and electrical resistivity because the thermal conductivity is modulated extrinsically by the organic matrix. As presented in this study, herein, the Bi<sub>2</sub>Te<sub>3</sub> particles, which are more resistive than Sb and Bi particles, presented lower  $R$  with the Au skins. This result suggests the Bi<sub>2</sub>Te<sub>3</sub> particles can potentially focus on mainly enhancing the Seebeck coefficient towards over ±200 μV/K in the correlation between the Seebeck coefficient and electrical resistivity<sup>[16]</sup>. Furthermore, in relation to the TE particles, we can additionally suppress the deposition of heat-conductive Au on the inside of particles by selecting void-less Bi<sub>2</sub>Te<sub>3</sub> particles. The void-less Bi<sub>2</sub>Te<sub>3</sub> particles are also beneficial in reducing a fluctuation on surface area for the planting and stabilizing the planting process for the mass production.

## CONCLUSIONS

Learning from OLEDs and DSCs, we have divided two of the property requirements for TE particles, namely, a high Seebeck coefficient and low interfacial resistance, into two material compositions of the Bi<sub>2</sub>Te<sub>3</sub> bodies and the Au skins, respectively. We then improved the TE power generation of the constructed module over two orders of magnitude more than that of the previous study to achieve 255 μW using the sticky TE materials of Bi<sub>2</sub>Te<sub>3</sub> particles covered by partial Au skins. For the next two orders of magnitude improvement to compete with the solid-state TE modules even in terms of power generation capacity, we have further suggested the advanced hierarchical design based on the module structure with high cell density at the macroscale, the thermally stable organic surroundings using thermal insulation foams as the sealants at the microscale, the electric resistance heating of Au or Ag skins to solder the TE particles at the nanoscale and void-less Bi<sub>2</sub>Te<sub>3</sub> particles enhancing the Seebeck coefficient at the atomic scale. In short, we can consider meeting the multiple complex requirements for mass production of flexible TE sheets by hierarchically hybridizing the multiple components serving for each requirement.

## DECLARATIONS

### Authors' contributions

Designed the study, performed data analysis and interpretation, and wrote the draft: Satoh N

Performed data acquisition and provided technical support: Otsuka M

Provided the best of knowledge and administrative support and added discussion to the received draft: Kawakita J, Mori T

### Availability of data and materials

Not applicable.

### Financial support and sponsorship

This report is based on results obtained from projects, JPNP14004 and JPNP20004, subsidized by the New Energy and Industrial Technology Development Organization (NEDO), Japan. This work was also supported by Japan Science and Technology Agency Mirai Program (JPMJMI19A1) and Public/Private R&D Investment Strategic Expansion Program (PRISM), Japan.

### Conflicts of interest

All authors declared that there are no conflicts of interest.

### Ethical approval and consent to participate

Not applicable.

### Consent for publication

Not applicable.

### Copyright

© The Authors 2022.

## REFERENCES

1. Petsagkourakis I, Tybrandt K, Crispin X, Ohkubo I, Satoh N, Mori T. Thermoelectric materials and applications for energy harvesting power generation. *Sci Technol Adv Mater* 2018;19:836-62. [DOI](#) [PubMed](#) [PMC](#)
2. Akinaga H. Recent advances and future prospects in energy harvesting technologies. *Jpn J Appl Phys* 2020;59:110201. [DOI](#)
3. Nandihalli N, Liu CJ, Mori T. Polymer based thermoelectric nanocomposite materials and devices: fabrication and characteristics. *Nano Energy* 2020;78:105186. [DOI](#)
4. Satoh N, Otsuka M, Ohki T, et al. Organic  $\pi$ -type thermoelectric module supported by photolithographic mold: a working hypothesis of sticky thermoelectric materials. *Sci Technol Adv Mater* 2018;19:517-25. [DOI](#) [PubMed](#) [PMC](#)
5. Satoh N, Otsuka M, Sakurai Y, et al. Sticky thermoelectric materials for flexible thermoelectric modules to capture low-temperature waste heat. *MRS Advances* 2020;5:481-7. [DOI](#)
6. Biswas K, He J, Blum ID, et al. High-performance bulk thermoelectrics with all-scale hierarchical architectures. *Nature* 2012;489:414-8. [DOI](#) [PubMed](#)
7. Liu Z, Mori T. Nanostructured bulk thermoelectric materials for energy harvesting. In: Wakayama Y, Ariga K, editors. System-materials nanoarchitectonics. Tokyo: Springer; 2022. pp. 199-231. [DOI](#)
8. Satoh N, Cho JS, Higuchi M, Yamamoto K. Novel triarylamine dendrimers as a hole-transport material with a controlled metal-assembling function. *J Am Chem Soc* 2003;125:8104-5. [DOI](#) [PubMed](#)
9. Satoh N, Nakashima T, Yamamoto K. Metal-assembling dendrimers with a triarylamine core and their application to a dye-sensitized solar cell. *J Am Chem Soc* 2005;127:13030-8. [DOI](#) [PubMed](#)
10. Satoh N, Han L. Chemical input and I-V output: stepwise chemical information processing in dye-sensitized solar cells. *Phys Chem Chem Phys* 2012;14:16014-22. [DOI](#) [PubMed](#)
11. Liu Z, Sato N, Gao W, et al. Demonstration of ultrahigh thermoelectric efficiency of  $\sim 7.3\%$  in Mg<sub>3</sub>Sb<sub>2</sub>/MgAgSb module for low-temperature energy harvesting. *Joule* 2021;5:1196-208. [DOI](#)
12. II-VI Marlow. Thermoelectric generator (TEG) modules. Available from: <https://ii-vi.com/product/thermoelectric-generator-teg-modules/> [Last accessed on 16 August 2022].
13. Liu Z, Gao W, Oshima H, Nagase K, Lee CH, Mori T. Maximizing the performance of n-type Mg<sub>3</sub>Bi<sub>2</sub> based materials for room-temperature power generation and thermoelectric cooling. *Nat Commun* 2022;13:1120. [DOI](#) [PubMed](#) [PMC](#)
14. Kim SJ, We JH, Cho BJ. A wearable thermoelectric generator fabricated on a glass fabric. *Energy Environ Sci* 2014;7:1959. [DOI](#)
15. Satoh N, Nakashima T, Yamamoto K. Metastability of anatase: size dependent and irreversible anatase-rutile phase transition in atomic-level precise titania. *Sci Rep* 2013;3:1959. [DOI](#) [PubMed](#) [PMC](#)
16. Yim W, Rosi F. Compound tellurides and their alloys for peltier cooling-A review. *Solid-State Electronics* 1972;15:1121-40. [DOI](#)